

**Investigation of the mechanics of the airfoil:  
application of machine learning in the noise  
prediction of NACA 0012**

Hanfeng Zhai

Shanghai Institute of Applied Mathematics and Mechanics,  
School of Mechanics and Engineering Science,  
Shanghai University

June 10, 2020

*Fluid physics on Flight*

## **Investigation of the mechanics of the airfoil: application of machine learning in the noise prediction of NACA 0012**

### **Abstract**

NACA 0012 is a typical airfoil widely applied for studies of fluid mechanics. The fluid stream on airfoil creates noise. The mechanism of airfoil noise is complicated. The concentration of the study is to investigate the noise of NACA 0012 based on the experimental database. The NACA airfoil is introduced in which related parameters and designation are shown as figures. The mechanism of airfoil encounters a free stream flow is given and introduced. Plus, based on simulation and obtained data, the mechanical distribution of the airfoil is presented in both the form of diagrams and simulation results. The attributes of the applied database are presented, where the data attributes are represented as figures. The mathematical basis of the decision tree and a linear regression model is demonstrated through equations. Hence, the calculation results of the decision tree and linear regression model is presented as the form of figures and formulas. Here, I applied a set of data trained for the model to verify the validity of both the decision tree and regression model. Simultaneously, a set of tested data is used in both the models to get the predicted noise of airfoil NACA 0012.

**Keywords:** computational fluid dynamics; machine learning; finite element method; airfoils; NACA0012

## Introduction

The application and study of airfoil started in the 20<sup>th</sup> century, in which the NACA airfoil, a collection and parameters' algorithm of airfoil created by NASA, is widely applied and studied by scholars. Computational fluid dynamics is also widely used in the study of airfoils, especially in determining the mechanical distribution and analytical refinement of airfoil design [2]. The dynamic motion and vortex distribution are also taken into consideration [3]. Similar works were then, coupled with wind tunnel test to investigate the wing-body effect [4]. The numerical study also investigates its ground effect focusing on the wing vortex [5]. The wing's noise effect and pollutant emission's effect is then be reviewed and discussed [6]. Most importantly, the morphology and its mechanical effect of NACA 0012 airfoil are discussed, which elucidate the important mechanism of airfoil's geometrical parameters on mechanics [7]. The material designation, which includes material and structural arrangement, contributes largely to the reduction of noise [8], which are discussed in this article. The computational mechanical coefficients (Lift, Drag, Moment) is calculated by investigating various parameters in the CFD process [9]. Taken the 3D wing as a whole, the algorithm for computational simulation methods is discussed and applied to different wing shape [10]. For what is more, certain optimization based on mechanical coefficients calculation is presented [11]. The complex essence of airfoil design is elucidated in detail considering fluid mechanics [12]. The detailed investigation of the CFD application on NACA 0012 is proposed in a methodology to harvest the benefits of camber morphing airfoils for small

unmanned aerial vehicle (SUAV) applications [13]. The fluid fields and mechanical coefficients are studied by inspecting the angle of attack ([14], [15]). The vibration and noise are generally mostly caused by the vortex. Airframe noise of engine vortex is studied by carrying out extensively noise control tests, which presents a few design concepts on the landing gear, high-lift devices, and whole aircraft are provided for advanced aircraft low-noise design [16]. Such vortex is also studied with regards to Reynold's number [17].

Taken consideration of the airfoil's noise, complex characters synergized the production of fluid noise, which is still in studying by scholars. Albeit the exact equation depicting the cause of noise does not exist, a significant amount of methods can be applied for noise prediction, including model describing the running of the engine [18]. Therefore, noise reduction potentials are thence be demonstrated through numerical method [19]. Experimental methods for noise detection is also presented with results of different noise reduction approaches [20]. Specific wing design could also reduce noise [21]. In fine, noise is very complicated and yet has no exact methods for the study.

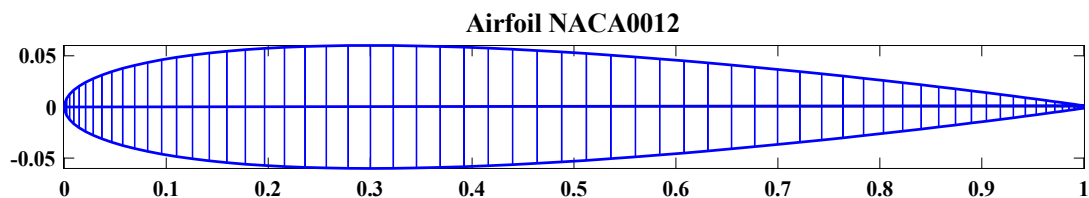
Notwithstanding, machine learning is born to solve complicated, knotty problems. Based on the database applied from experiments of airfoil NACA 0012 containing noise and related attributes' data [1], Brooks *et al.* [22] presents predictions of the airfoil noise based on previous data and methodologies. Then, a neural network study for noise prediction is presented ([23], [24]).

## Method

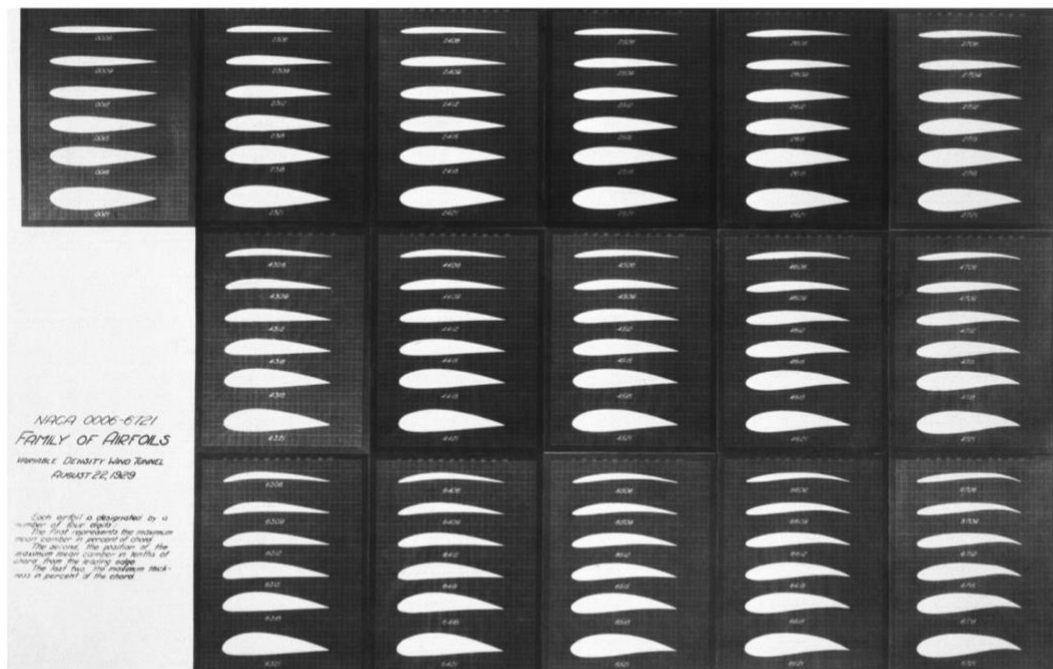
### NACA 0012

The NACA airfoils are airfoil shapes for aircraft wings developed by the National Advisory Committee for Aeronautics (NACA). The parameters in the numerical code can be entered into equations to precisely generate the cross-section of the airfoil and calculate its properties. [25]

The schematic view of airfoil NACA 0012 is shown as in Figure 1, in which the geometrical parameters is obtained from *Airfoil-Tools* [26].

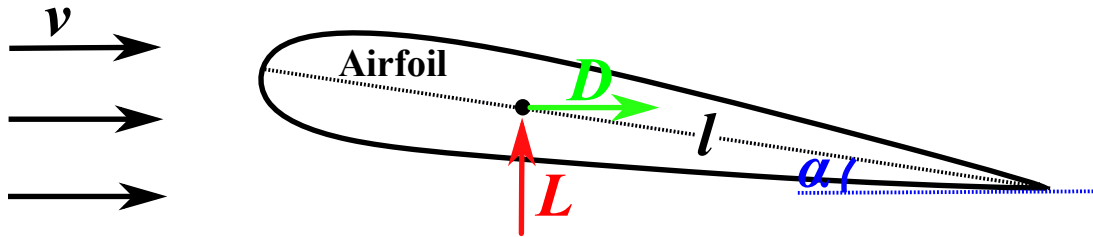


**Fig. 1** Schematic illustration of airfoil [NACA0012] morphology.





**Fig. 2** The collection of NACA airfoil [25].

When encountered with free stream flow, the airfoil will experience lift and drag force, which magnitude is determined by velocity ( $v$ ), angle of attack ( $\alpha$ ), etc. as shown in Figure 3. Such mechanical distribution will hence be analyzed through simulation and decent diagrams.



**Fig. 3** Schematic view for the mechanical distribution on airfoil free stream velocity.

Plus, on account of the air friction, boundary layer detachment, vibration, etc. the airfoil will generate noise of different magnitudes. The mechanisms of such noise are complex. Thus, with the application of machine learning, we can discern certain mechanisms under the noise generation based on the airfoil experimental database.

<b>Input Dataset</b> 	<b>Frequency</b> [Hertz]	
	<b>Angle of attack</b> [degrees]	
	<b>Chord length</b> [meters]	1503 (data)
	<b>Free-stream velocity</b> [meters/second]	×
	<b>Suction side displacement thickness</b> [meters]	5 (sets)
<b>Output Dataset</b> 	<b>Scaled sound pressure level</b> [decibels]	1503 (data)

**Tab. 1** The basic information and attributes of the airfoil dataset.

The attributes of the database are shown in Table 1, from which one could obtain that there are five attributes that are taken into consideration in the experiments: Frequency, Angle of Attack, ..., Suction side displacement thickness. The value of these attributes with their relation with Scaled sound pressure level is shown in Figure 4, where Scaled sound indicates the airfoil's noise.

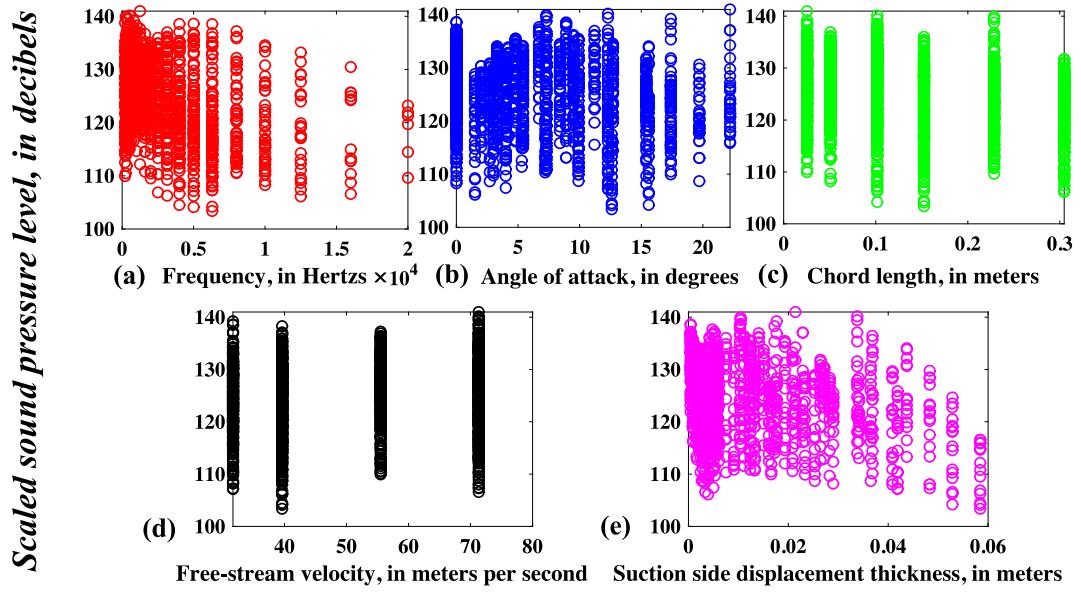


**Fig. 4** The diagram of data attributes of the airfoil data. (a) Sound Pressure-Frequency diagram. (b) Sound Pressure-Attack Angle diagram. (c) Sound Pressure-Chord Length diagram. (d) Sound Pressure-Velocity diagram. (e) Sound Pressure-Displacement Thickness diagram.

### Decision Tree

When estimating the purity of data sets, we often choose information entropy as a metric. First, let us first set  $D$  to represent the database, the proportion of the  $k$ th sample in the data is  $p_k (k=1, 2, \dots, |y|)$ , then the information entropy  $D$  can now be defined as

$$Ent(D) = - \sum_{k=1}^{|y|} p_k \log_2 p_k \quad (1)$$

In which the smaller the value of  $Ent(D)$ , the higher the purity of entropy  $D$ .

Now assume that the discrete attribute  $a$  has  $V$  possible values  $\{a_1, a_2, \dots, a_V\}$ , and now divide the sample set  $D$  for the general attribute  $a$ , then there will be  $V$  branch nodes (the  $v$ th branch node contains  $D$  where the sample with the value  $a_v$  on the attribute  $a$  is denoted as  $D_v$ ). based on the entropy definition, the number of different samples included in different branches can be considered where the branch node is given as  $|D^v|/|D|$ . then it can be inferred that the samples' numbers correlate with the branch node influence. Hence, the information gain of attribute  $a$  for sample  $D$  can be calculated:

$$Gain(D, a) = Ent(D) - \sum_{v=1}^V \frac{|D^v|}{D} Ent(D^v) \quad (2)$$

When selecting classification indices for the sample set, there are many classification methods. In this paper, Gini index are used for classification and calculation. First, the Gini index is applied to analyze the purity of the data set  $D$ :

$$Gini(D) = \sum_{k=1}^{|y|} \sum_{k' \neq k} p_k p_{k'} \quad (3)$$

Among which the  $Gini(D)$  are randomly drawing two samples from the data set  $D$ , and their categories are respectively marked or represent different probabilities.

Therefore, the smaller the calculated  $Gini(D)$  value, the higher purity of the data set

$D$ , where the attribute  $a$  Gini index is defined as

$$Gini\_index(D, a) = \sum_{v=1}^V \frac{|D^v|}{D} Gini(D^v) \quad (4)$$

In the paper, to simplify the calculation process, I deviate the scaled sound pressure in to two values, 0 and 1, which is distinguished by the mean value of sound



pressure. According to the attributes in Table 1, the equation of the decision tree calculation is shown in Equation 5.

$$\begin{cases}
 Gini\_index(D, Frequency) = \frac{value_1(v)}{1503} \left\{ 2 \cdot \frac{value_1(noise\_1)}{value_1} \cdot \left( 1 - \frac{value_1(noise\_1)}{value_1} \right) \right\} \\
 + \frac{value_2}{1053} \left\{ 2 \cdot \frac{value_2(noise\_1)}{value_2} \cdot \left( 1 - \frac{value_2(noise\_1)}{value_2} \right) \right\} + \dots + \frac{value_n}{1503} \left\{ 2 \cdot \frac{value_n(noise\_1)}{value_n} \cdot \left( 1 - \frac{value_n(noise\_1)}{value_n} \right) \right\} \\
 Gini\_index(D, Angle of attack) = \frac{v_1(angle\ of\ attack)}{1503} \left\{ 2 \cdot \frac{v_1(n\_1)(\alpha)}{v_1(\alpha)} \cdot \left( 1 - \frac{v_1(n\_1)}{v_1} \right) \right\} + \dots \\
 Gini\_index(D, Chord length) = \frac{v_1(l)}{1503} \left\{ 2 \cdot \frac{v_1(noise\_1)(l)}{v_1} \cdot \left( 1 - \frac{v_1(n\_1)}{v_1} \right) \right\} + \dots \\
 Gini\_index(D, Free stream velocity) = \frac{v_1(v)}{1503} \left\{ 2 \cdot \frac{v_1(n\_1)(v)}{v_1} \cdot \left( 1 - \frac{v_1(n\_1)(v)}{v_1} \right) \right\} + \dots \\
 Gini\_index(D, Suction side displacement thickness) = \frac{v_1(\delta)}{1503} \left\{ 2 \cdot \frac{v_1(n\_1)(\delta)}{v_1} \cdot \left( 1 - \frac{v_1(n\_1)(\delta)}{v_1} \right) \right\} + \dots
 \end{cases} \quad (5)$$

### **Linear Regression**

Initially, for a dataset with  $d$  attributes (independent variables), where we express as  $\mathbf{x} = (x_1; x_2; \dots; x_d)$ . Where  $x_i$  is the value of  $x$  in the  $i$ th attribute. Hence, a linear model for function can be predicted by building a linear model

$$f(\mathbf{x}) = \omega_1 x_1 + \omega_2 x_2 + \dots + \omega_d x_d + b \quad (6)$$

For the multiple linear regression problem of the data set  $D$  with  $d$  attributes, we use the general vector form to express

$$f(\mathbf{x}) = \boldsymbol{\omega}^T \mathbf{x}_i + b, \text{ where } f(\mathbf{x}_i) \cong y_i \quad (7)$$

Subsequently, we can use the least square method to estimate  $\boldsymbol{\omega}$  and  $b$ . For convenience, the vector form  $\hat{\boldsymbol{\omega}} = (\boldsymbol{\omega}; b)$  is introduced. Therefore, the dataset  $D$  can be represented as a matrix  $\mathbf{X}$  of size  $m \times (d + 1)$ , where each row corresponds to an example, and the top  $d$  elements of the row correspond to  $d$  attribute values in the instance, the element value in the last row is always 1.

$$\mathbf{X} = \begin{pmatrix} x_{11} & x_{12} & \dots & x_{1d} & 1 \\ x_{21} & x_{22} & \dots & x_{2d} & 1 \\ \dots & \dots & \dots & \dots & \dots \\ x_{m1} & x_{m2} & \dots & x_{md} & 1 \end{pmatrix} = \begin{pmatrix} \mathbf{x}_1^T & 1 \\ \mathbf{x}_2^T & 1 \\ \dots & \dots \\ \mathbf{x}_m^T & 1 \end{pmatrix} \quad (8)$$

in which the attribute  $\mathbf{y}$  takes the form

$$\mathbf{y} = (y_1; y_2; \dots; y_m) \quad (9)$$

We set the vector  $\hat{\boldsymbol{\omega}}^*$  as given:

$$\hat{\boldsymbol{\omega}}^* = \underset{\hat{\boldsymbol{\omega}}}{\operatorname{argmin}} (\mathbf{y} - \mathbf{X}\hat{\boldsymbol{\omega}})^T (\mathbf{y} - \mathbf{X}\hat{\boldsymbol{\omega}}) \quad (10)$$

Now we set  $E_{\hat{\boldsymbol{\omega}}} = (\mathbf{y} - \mathbf{X}\hat{\boldsymbol{\omega}})^T (\mathbf{y} - \mathbf{X}\hat{\boldsymbol{\omega}})$ , by derivation of  $\hat{\boldsymbol{\omega}}$  one get:

$$\frac{\partial E_{\hat{\boldsymbol{\omega}}}}{\partial \hat{\boldsymbol{\omega}}} = 2\mathbf{X}^T (\mathbf{X}\hat{\boldsymbol{\omega}} - \mathbf{y}) \quad (11)$$

Let the value of Equation 11 be zero, one get the optimal solution of  $\hat{\boldsymbol{\omega}}$ . When

$\mathbf{X}^T \mathbf{X}$  is a full rank matrix and a positive definite matrix, let  $\frac{\partial E_{\hat{\boldsymbol{\omega}}}}{\partial \hat{\boldsymbol{\omega}}}$  be zero one get:

$$\hat{\boldsymbol{\omega}}^* = (\mathbf{X}^T \mathbf{X})^{-1} \mathbf{X}^T \mathbf{y} \quad (12)$$

where  $(\mathbf{X}^T \mathbf{X})^{-1}$  be the inverse matrix of  $\mathbf{X}^T \mathbf{X}$ . Let  $\hat{\mathbf{x}}_i = (\mathbf{x}_i; 1)$ , hence eventually

one get the linear regression model:

$$f(\hat{\mathbf{x}}_i) = \hat{\mathbf{x}}_i^T (\mathbf{X}^T \mathbf{X})^{-1} \mathbf{X}^T \mathbf{y} \quad (13)$$

For the estimated dataset specifically, the  $\mathbf{X}$  matrix is given considering the five attributes of the dataset:

$\mathbf{X}_{variables}$

$$= \begin{pmatrix} \text{Frequency} & \text{Attack Angle} & \text{Chord length} & \text{Free velocity} & \text{Suction displacement} \\ value_{v1} & value_{\alpha1} & value_{l1} & values_{v1} & value_{\delta1} \\ \dots & \dots & \dots & \dots & \dots \\ value_{v1503} & value_{\alpha1503} & value_{l1503} & values_{v1503} & value_{\delta1503} \end{pmatrix} \quad (14)$$

Similarly, the  $\mathbf{y}$  vector is given based on the dataset as:

$$\mathbf{y}_{Scaled \text{ sound pressure level}} = (value_1; value_2; \dots; value_{1503}) \quad (15)$$

## Results

### *Mechanical Distribution*

Based on the preceding introduction of airfoil's mechanical distribution, one could carry out a simulation of NACA 0012 in thence obtain its pressure and velocity distribution, which are shown in Figure 5 and Figure 6, respectively.

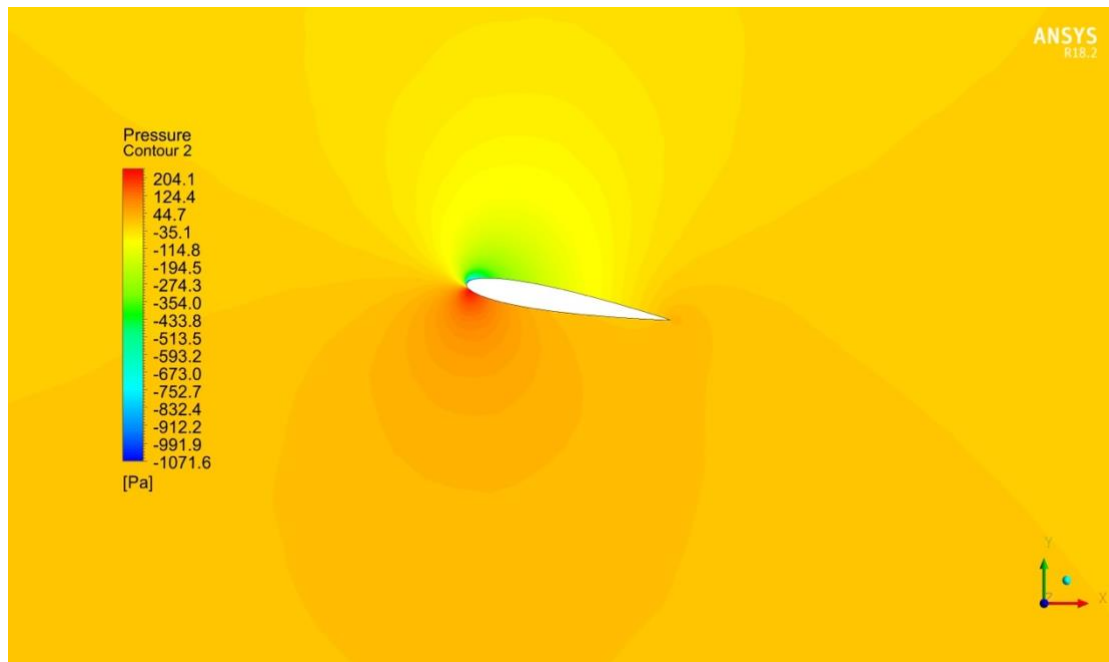


**Fig. 5** The simulation results of the pressure on airfoil [NACA0012].

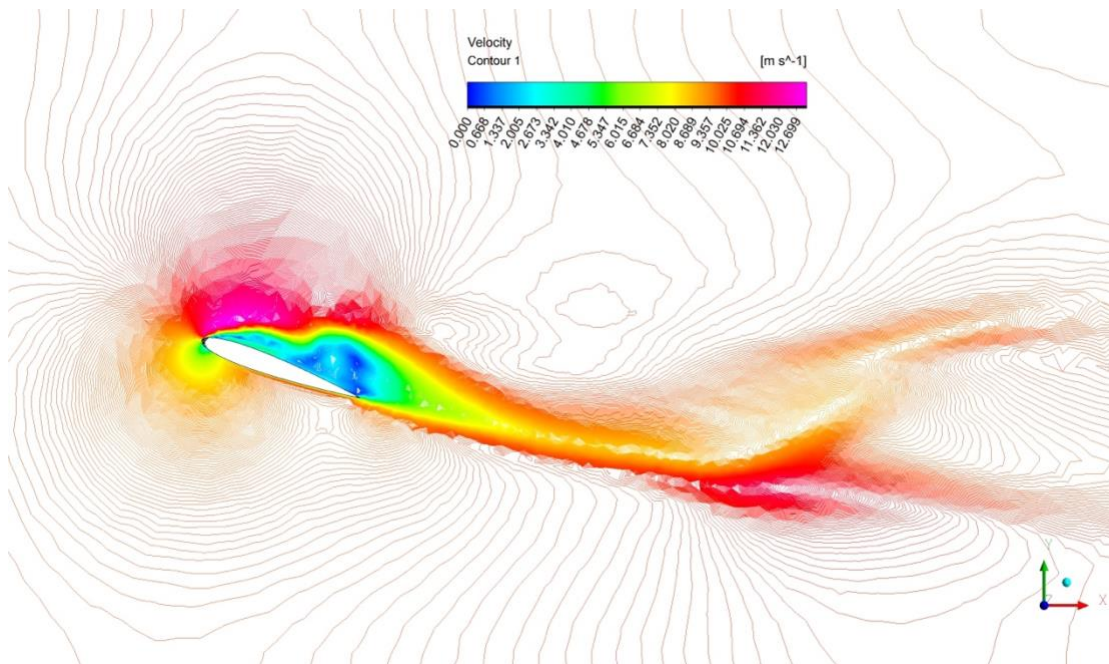


**Fig. 6** The simulation results of the velocity on airfoil [NACA0012].

From such distribution in Figure 5, one could deduce that the pressure on the lower surface is higher than which on the upper surface, which explains the lift force on an airfoil with the existence of angle of attack. Similarly, with the estimation of velocity distribution, one could observe a vortex that exists on the upper surface of the airfoil, in which velocity value is approximately zero indicating the drift-away of the boundary layer.

As introduced in the preceding chapter, there are lift, drag, and the moment on the airfoil when encountered free stream flow (Figure 3). These mechanical variables are denoted by dimensionless coefficients  $C_L$ ,  $C_D$ ,  $C_M$ , respectively. They correlate to the angle of attack ( $\alpha$ ), and Reynold's number ( $Re$ ). The relations of these mechanical coefficients to  $\alpha$  and  $Re$  is shown in diagrams (Figure 7).

### Airfoil NACA0012

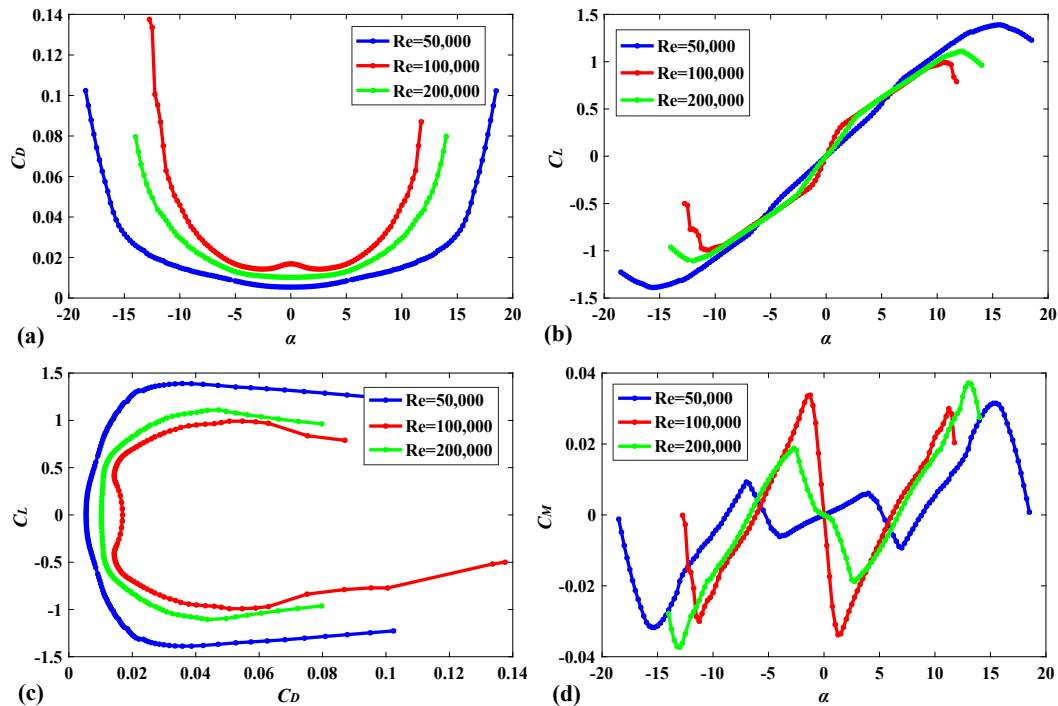


**Fig. 7** Mechanical distribution of the airfoil [NACA0012]. (a) The  $\alpha$ - $C_D$  diagram. (b) The  $\alpha$ - $C_L$  diagram. (c) The  $C_D$ - $C_L$  diagram. (d) The  $\alpha$ - $C_M$  diagram. In which  $\alpha$  is the angle of attack,  $C_D$  is the drag coefficient,  $C_L$  is the lift coefficient,  $C_M$  is the moment coefficient.

From Figure 7 one can observe that NACA 0012 mechanical coefficients generally have a complicated relation to  $\alpha$  and  $Re$ . The drag coefficient is the highest when  $Re = 100,000$  compared to applied  $Re$ . The coefficients fluctuate with no clear positive or negative correlation presented.

### Decision Tree

Based on the Gini index as mentioned (Equation 4). The decision tree judging the dataset with the sound pressure value of 0 and 1 can be obtained through the given algorithm and presented as schematic as shown in Figure 8.

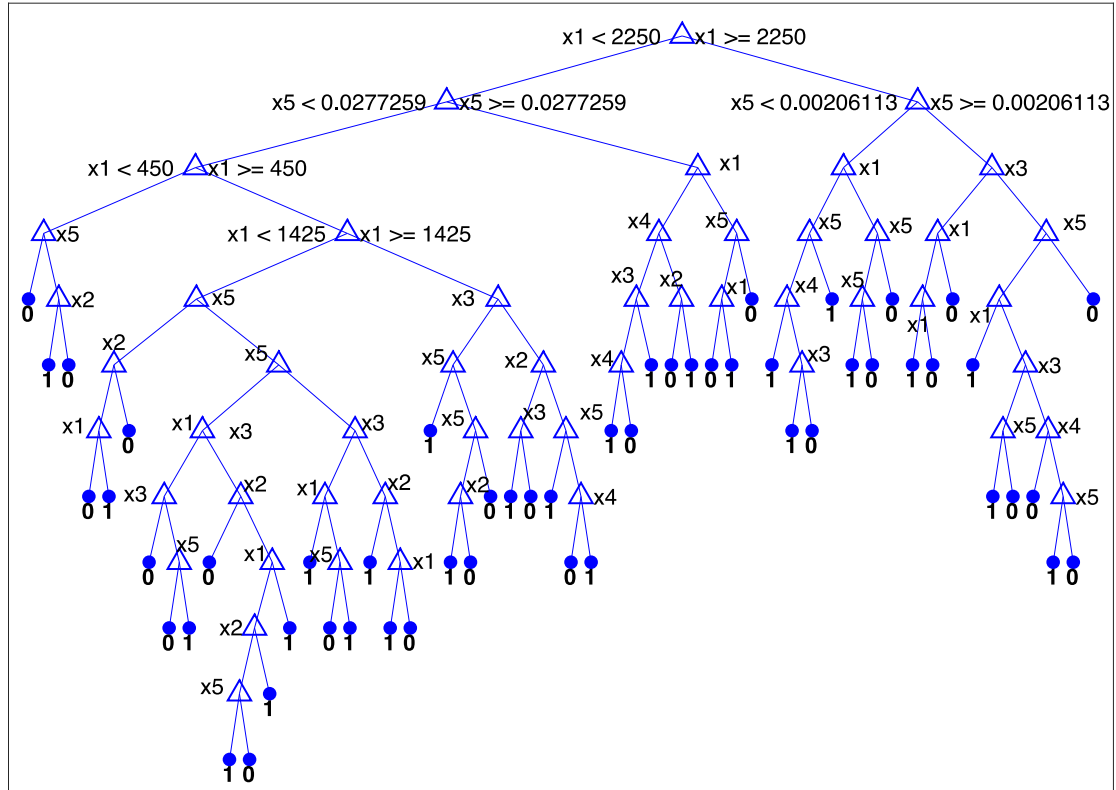


**Fig. 8** Schematic view for the decision tree calculated from the dataset.

The presented schematic view shows how the attributes in the dataset help us assess the value of the sound pressure (0 and 1), in which  $x_1, x_2, \dots, x_5$  represents the attributes of Frequency, Angle of Attack, ..., Suction displacement, respectively. The

decision tree also indicates that a robust correlation of the attributes in the dataset as the generally numerous branches.

### ***Linear Regression***

As presented (Equation 13) we already attain the relation between the input data attributes and the sound pressure (noise), a linear regression model could be built with the algorithms as presented in Figure 9. As shown in the figure the model could be simplified as an equation:  $y = 151.563x$ , in which  $x$  contains information of the tested variables.

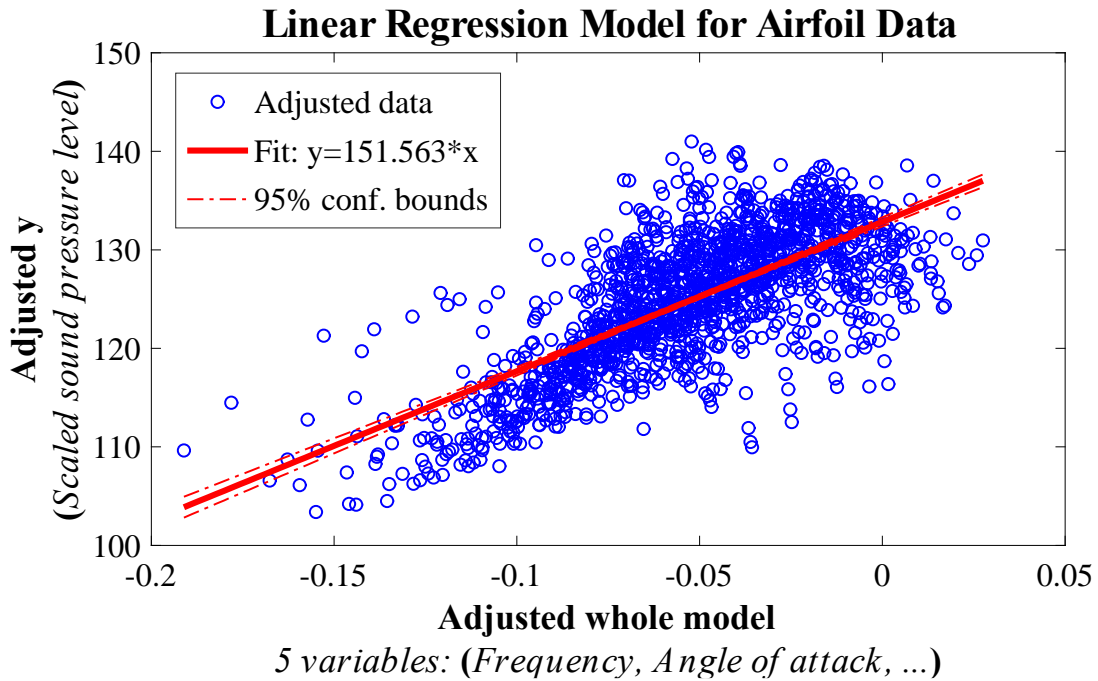


**Fig. 9** Fitting diagram of linear regression model fitted for airfoil dataset.

Based on the algorithms, we can build two linear regression models of the dataset. One is a perfectly linear model as shown in Table 1, in which the relation of the five variables to the sound scaled pressure is perfectly linear. In the table the variables  $x_1, x_2, \dots, x_5$  represents the attributes of Frequency, Angle of Attack, ..., Suction displacement, respectively.

Linear regression model:  $y \sim 1 + x_1 + x_2 + x_3 + x_4 + x_5$

	Estimate	SE	tStat	pValue
(Intercept)	132.833805778378	0.544700692398831	243.865681891069	0
x1	-0.00128220710890557	4.21054737495061e-05	-30.4522665279502	6.42181698991263e-159
x2	-0.421911705948041	0.0388960909748539	-10.8471492989052	1.92337642119333e-26
x3	-35.6880012257975	1.63043191185934	-21.8886792917952	2.28683899975858e-92
x4	0.0998540448518054	0.00813225943082764	12.2787579148398	4.34063619837972e-33
x5	-147.30051877787	15.0146684410392	-9.81044099350586	4.61724441831751e-22

**Tab. 2** Calculation results for linear regression model fitted for airfoil dataset.

Based on the parameters shown in Table 1, one get the linear model of the scaled sound pressure representing in equation:

$$P_{sound} = -1.28 \times 10^{-3} \nu - 4.22 \times 10^{-1} \alpha - 35.69l + 9.99 \times 10^{-2} v - 1.47 \times 10^2 \delta \quad (16)$$

In which  $\nu$  is the Frequency,  $\alpha$  is the angle of attack,  $l$  is the Chord length,  $v$  is the Free-stream velocity,  $\delta$  is the Suction side displacement thickness;  $P_{sound}$  is the Scaled sound pressure level.

Howbeit as shown before (Figure 4) one can deduce that the relation of the variables to the sound pressure is more complex than perfectly linear. Thence we implemented a coupled linear regression model.

Linear regression model:  $y \sim 1 + x_2 + x_1 \cdot x_3 + x_1 \cdot x_5 + x_3 \cdot x_4 + x_4 \cdot x_5$

	Estimate	SE	tStat	pValue
(Intercept)	131.107551175829	0.83173887119001	157.630664764107	0
x1	-0.000207045198598631	6.57024552883535e-05	-3.15125511961396	0.00165798968352487
x2	-0.263028545763508	0.0348685726211137	-7.54342739009164	7.91349422142312e-14
x3	-26.5717945260154	4.15373708361991	-6.39708146931113	2.11398122204992e-10
x4	0.0393744358643762	0.0152452412749828	2.58273615708457	0.00989645186584277
x5	-147.282535654558	30.7278529952379	-4.79312810033891	1.8056401215327e-06
x1:x3	-0.00507495827908918	0.000354198419409863	-14.328009389609	1.00696658701296e-43
x1:x5	-0.0669843797917566	0.00406323583715607	-16.4854767176498	3.17903990160932e-56
x3:x4	0.244926722625617	0.0777389551739563	3.15063049249305	0.00166151544042849
x4:x5	2.09267395321099	0.555892284068762	3.7645313906752	0.000173330833429639

**Tab. 3** Calculation results for optimized linear regression model fitted for airfoil dataset.

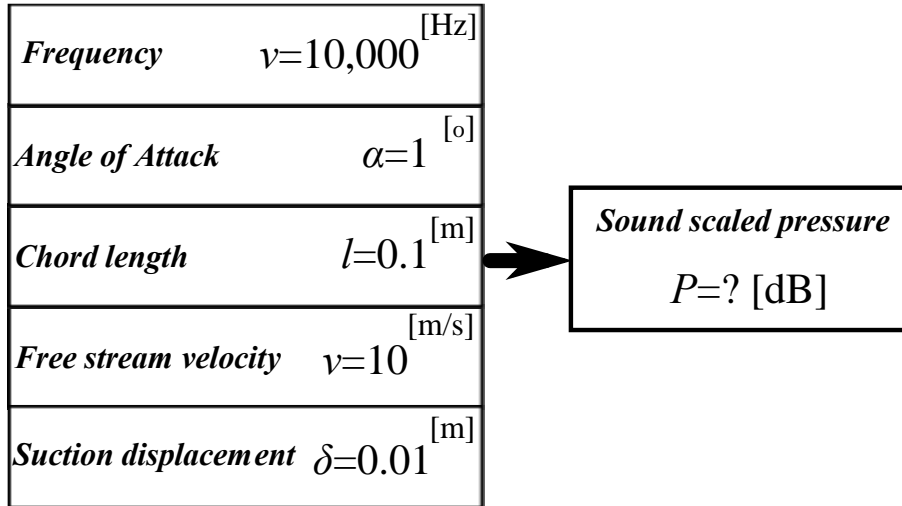
Based on such the equation could be written as:

$$P_{sound} = 1 - 0.26\alpha - 5.07 \times 10^{-3}\nu l - 6.70 \times 10^{-2}\nu\delta + 2.45 \times 10^{-1}l\nu + 2.09\nu\delta \quad (17)$$

In which  $\nu$  is the Frequency,  $\alpha$  is the angle of attack,  $l$  is the Chord length,  $\nu$  is the Free-stream velocity,  $\delta$  is the Suction side displacement thickness;  $P_{sound}$  is the Scaled sound pressure level.

### Noise Prediction

Therefore, as the model obtained, we could implement tested data to predict the noise of airfoil NACA 0012. With regard to the range of data in the trained dataset, I set a group of data to predict the possible noise with existed input data.



**Tab. 4** The process of obtained the predicted sound noise of airfoil NACA 0012.

When implemented on the obtained decision tree (Figure 8), distinguished by the attributes' data of  $x_1$ ,  $x_3$  and  $x_5$  (Frequency, Chord length, Suction displacement), we obtain the final judgement of  $x_5$  (Sound pressure) is 0. Hence, we can conclude the noise of such data is below the mean value, which is  $P_{sound} \leq 125.721$  [dB].

When implemented such data on perfect linear regression (Equation 16) one obtain  $P_{sound} = 115.5466$  [dB]. The coupled linear regression (Equation 17) one



obtain  $P_{sound} = 137.7693$  [dB]. The predicted noise of the coupled linear regression does not correlate with the decision tree judgement, which indicate that errors exists in the coupled linear tree and the accuracy is not high with the input data.

## Conclusion

NACA 0012 is a classical airfoil (Figure 1) created by NASA (Figure 2) used for research in the field of fluid mechanics. The airfoil will take lift, drag forces and moment undergoing free stream velocity (Figure 3). The mechanical distribution on the airfoil could be investigated through decent simulations (Figure 5 and Figure 6) and the drag, lift and moment coefficients with their relations to angle of attack and Reynold's number could be presented in diagrams (Figure 7).

Specifically, the free flow interacting with the airfoil will generate noise that can be represented by the sound scaled pressure. The mechanism behind such interaction is complex and there are hardly widely accepted equations representing such relation. Notwithstanding with the application of machine learning, which including decision tree (Equation 1-Equation 5) and linear regression (Equation 6-Equation 15) we could discern such relation. An experimental dataset containing information of NACA 0012 related mechanical variables and sound pressure is implemented for the algorithms (Table 1, Figure 4). With the application of decision tree algorithm, a schematic diagram of the decision tree could be obtained (Figure 8). Plus, the perfectly and coupled linear regression model is presented as given (Table 2, Table 3, Equation 16, Equation 17). Based on such results, we can implement a set of testing data to predict the possible value of the sound pressure. When inputting a set of data containing

certain values of mechanical variables (Table 4), we obtain the predicted level of noise from decision tree is 0, which mean it below the mean value ( $P_{sound} \leq 125.721$  [dB]). With the application of perfectly linear model, the predicted sound scaled pressure is  $P_{sound} = 115.5466$  [dB]. The predicted sound pressure for coupled linear regression model is  $P_{sound} = 137.7693$  [dB].

## **Discussion**

The mechanism of the airfoil's noise is still complex and yet to be depicted by detailed equations. Howbeit, we present a possible application of noise prediction by inputting the airfoil mechanical data. Albeit errors more or less existed as distortions shown in the results of the decision tree and coupled linear regression model, the method still provide an approximate scale of the noise generated by the airfoil. The pedigree of the noise includes shift-away of the boundary layer, vortex collision, etc. These phenomena are arduous to be depicted by equations when they are coupled with each other.

In fine, the presented methodologies could provide guidelines and decent insights for manufacturing and designation of airfoil, further, plane wing.

## **Acknowledgements**

The airfoil's dataset [NACA0012] implemented for linear regression and the decision tree training is obtained from UCI Machine Learning Repository from Dr Roberto Lopez [\[Dua ,D. et al 2019\]](#). The simulation of airfoil NACA 0012 is generated from B. Liang and the contribution of the modelling is greatly acknowledged.

## References

- [1] Dua, D. and Graff, C. (2019). UCI Machine Learning Repository [<http://archive.ics.uci.edu/ml>]. Irvine, CA: University of California, School of Information and Computer Science.
- [2] Antonio Fazzolari, Dott. in Fisica. An aero-structure adjoint formulation for efficient multidisciplinary wing Optimization. Conference Paper · January 2005. Datum der Promotion (Tag der mdl. Prüfung): 12.12.2005.
- [3] D. Funda Kurtulus, Alain Farcy, Nafiz Alemdaroglu. Unsteady Aerodynamics of Flapping Airfoil in Hovering Flight at Low Reynolds Numbers · January 2005. DOI: 10.2514/6.2005-1356
- [4] A.R. Davari, M.R. Soltani, F. Askari, H.R. Pajuhande. Effects of wing geometry on wing-body-tail interference in subsonic flow. *Scientia Iranica B* (2011) 18 (3), 407–415. doi:10.1016/j.scient.2011.05.031
- [5] Hui Liang, Xijun Wang, Li Zou, Zhi Zong. Numerical study of two-dimensional heaving airfoils in ground effect. *Journal of Fluids and Structures* 48 (2014) 188–202. dx.doi.org/10.1016/j.jfluidstructs.2014.02.009
- [6] W.R. Graham, C.A. Hall, M. Vera Morales, The potential of future aircraft technology for noise and pollutant emissions reduction, *Transport Policy*, Volume 34,2014,Pages 36-51,ISSN 0967-070X
- [7] J.H.S. Fincham, M.I. Friswell. Aerodynamic optimisation of a camber morphing aerofoil. *Aerospace Science and Technology* 43 (2015) 245–255. dx.doi.org/10.1016/j.ast.2015.02.023
- [8] Wang, Xiaole, et al. Reduction of aircraft engine noise by covering surface acoustic metamaterials on sidewalls[C]. *Proceedings of the 24th International Congress on Sound and Vibration (ICSV)*, London, UK. 2017.
- [9] Yunpeng Qin ,Peiqing Liu,Qiulin Qua,Tianxiang Hua.Wing/canard interference of a close-coupled canard configuration in static ground effect .*Aerospace Science and Technology*.DOI: <http://dx.doi.org/10.1016/j.ast.2017.06.012>
- [10] Johan Boutet, Grigorios Dimitriadis. Unsteady Lifting Line Theory Using the Wagner Function for the Aerodynamic and Aeroelastic Modeling of 3D Wings. *Aerospace* 2018, 5, 92. doi:10.3390/aerospace5030092
- [11] Nathanael J. Curiale, David W. Zingg. Morphing Wings: A Study Using Aerodynamic Shape Optimization. *AIAA 2018-1910*. Session: Aerodynamic Shape Optimization II. 7 Jan 2018 doi.org/10.2514/6.2018-1910.
- [12] Sun J Q , Xiong F R , Schütze, Oliver, et al. Multi-objective Optimal Airfoil Design[J]. *Cell Mapping Methods*. 2019, 10.1007/978-981-13-0457-6(Chapter 12): 191-202.
- [13] T Rajesh Senthil Kumar, Sivakumar Venugopal, Balajee Ramakrishnananda, S. Vijay. Aerodynamic Performance Estimation of Camber Morphing Airfoils for Small

- Unmanned Aerial Vehicle. *J. Aerosp. Technol. Manag.*, São José dos Campos, v12, e1420, 2020.
- [14] D. Durante, E. Rossi, A. Colagrossi. Bifurcations and chaos transition of the flow over an airfoil at low Reynolds number varying the angle of attack. *Journal Pre-proof*. DOI: <https://doi.org/10.1016/j.cnsns.2020.105285>
- [15] Lorenzo Battisti, Luca Zanne, Marco Raciti Castelli, Alessandro Bianchini, Alessandra Brighenti. A generalized method to extend airfoil polars over the full range of angles of attack. *Renewable Energy*. DOI: <https://doi.org/10.1016/j.renene.2020.03.15>
- [16] Li Yong, Wang Xunnian, Zhang Dejiu. Control strategies for aircraft airframe noise reduction. *Chinese Journal of Aeronautics*. DOI: <http://dx.doi.org/10.1016/j.cja.2013.02.001>
- [17] Suwin Slesongsom, Sujin Bureerat. Aerodynamic Reduced-Order Modeling without Static Correction Requirement Based on Body Vortices. *Article in Journal of Engineering*. April 2013. DOI: 10.1155/2013/326496
- [18] Antonio Filippone, Aircraft noise prediction, *Progress in Aerospace Sciences*, Volume 68, 2014, Pages 27-63, ISSN 0376-0421
- [19] Antonio Filippone, Options for aircraft noise reduction on arrival and landing, *Aerospace Science and Technology*, Volume 60, 2017, Pages 31-38, ISSN 1270-9638
- [20] Misol, Malte. Experiments on noise reduction in aircraft with active sidewall panels[C]. *Proceedings of the 25th International Congress on Sound and Vibration (ICSV)*, Hiroshima, JP. 2018.
- [21] Heininen, Arttu, et al. Equations of State in Fighter Aircraft Oleo-pneumatic Shock Absorber Modelling[C]. *FT2019. Proceedings of the 10th Aerospace Technology Congress*, October 8-9, 2019, Stockholm, Sweden. No. 162. Linköping University Electronic Press,
- [22] T.F. Brooks, D.S. Pope, and A.M. Marcolini. Airfoil self-noise and prediction. Technical report, NASA RP-1218, July 1989.
- [23] K. Lau. A neural networks approach for aerofoil noise prediction. Master's thesis, Department of Aeronautics. Imperial College of Science, Technology and Medicine (London, United Kingdom), 2006.
- [24] R. Lopez. Neural Networks for Variational Problems in Engineering. PhD Thesis, Technical University of Catalonia, 2008.
- [25] NACA Airfoil. Wikipedia.
- [26] NACA 0012 AIRFOILS (n0012-il). AirfoilTools.